Measurement report: High Contributions of Halocarbon and Aromatic Compounds to Atmospheric VOCs in Industrial Area

Ahsan Mozaffar [1,2,3], Yan-Lin Zhang [1,2,3*], Yu-Chi Lin[1,2,3], Feng Xie [1,2,3], Mei-Yi Fan [1,2,3], and Fang Cao [1,2,3]

[1]Yale-NUIST Center on Atmospheric Environment, International Joint Laboratory on Climate and Environment Change, Nanjing University of Information Science and Technology, Nanjing, 210044, China.

[2]Key Laboratory Meteorological Disaster; Ministry of Education & Collaborative Innovation Center on Forecast and Evaluation of Meteorological Disaster, Nanjing University of Information Science and Technology, Nanjing, 210044, China.

[3]Jiangsu Provincial Key Laboratory of Agricultural Meteorology, College of Applied Meteorology, Nanjing University of Information Science & Technology, Nanjing 210044, China.

Correspondence to: Yan-Lin Zhang (dryanlinzhang@outlook.com)

Abstract. Volatile organic compounds (VOCs) are key components of tropospheric chemistry. We investigated ambient VOCs in an industrial area in Nanjing, China between July 2018 and May 2020. The sum of the suite of measured VOCs (TVOCs) concentrations was 59.8±28.6 ppbv during the investigation period. About twice the TVOCs concentrations were observed in the autumn (83±20 ppbv) and winter (77.5±16.8 ppbv) seasons compared to those in spring (39.6±13.1 ppbv) and summer (38.8±10.2 ppbv). In previous studies in Nanjing, oxygenated-VOCs (OVOCs) and halocarbons were not measured, the current TVOCs concentration without halocarbons and OVOCs was similar to the previous investigation in the same study area; however, it was 2-folds higher than the one reported in the nonindustrial suburban area of Nanjing. Due to the industrial influence, the halocarbons VOC-group (14.3±7.3 ppbv, 24%) was the second largest contributor to the TVOCs after alkanes (21±7 ppbv, 35%), which is in contrast with the previous studies in Nanjing and also in almost other regions in China. Relatively high proportions of halocarbons and aromatics were observed in autumn (25.7 and 19.3%, respectively) and winter (25.8 and 17.6%, respectively) compared to those in summer (20.4 and 11.8%,

respectively) and spring (20.3 and 13.6%, respectively). According to the potential source contribution function (PSCF), short-distance transports from the surrounding industrial areas and cities were the main reason for the high VOC concentration in the study area. According to positive matrix factorization (PMF) model results, vehicle-related emissions (33-48%) contributed to the major portion of the ambient VOC concentrations. Aromatics followed by alkenes were the top contributors to the loss rate of OH radicals (L_{OH}) (37 and 32%, respectively). According to the empirical kinetic modelling approach (EKMA) and relative incremental reactivity (RIR) analysis, the study area was in the VOC-sensitive regime for ozone (O_3) formation during all the measurements seasons. Therefore, alkenes and aromatics emissions from automobiles need to be decreased to reduce secondary air pollution formation in the study area.

1 Introduction

Air pollution characterized by severe ozone (O_3) and haze pollution is a big problem in urban and industrial areas in China (He et al., 2019; Hui et al., 2018; Tan et al., 2018; Jia et al., 2016; Feng et al., 2016; Hui et al., 2019). In recent years, O_3 concentrations above the national standard and severe haze events have been frequently reported (He et al., 2019; Hui et al., 2019; Sheng et al., 2018; Feng et al., 2016; Tan et al., 2018; Jia et al., 2016). As a precursor of O_3 and secondary organic aerosol (SOA), volatile organic compounds (VOCs) are largely responsible for the severe air pollution in China (Song et al., 2018; Hui et al., 2019; Hui et al., 2018; He et al., 2019). Unfortunately, anthropogenic VOC emissions have been increasing over the last two decades in China, and they are expected to do so in the future (Mozaffar & Zhang, 2020, and references therein).

Atmospheric VOC has plenty of sources; it can be emitted from various anthropogenic and biogenic sources. Besides, it can also be formed in the atmosphere. Anthropogenic VOC sources mainly include industrial emissions, vehicle exhaust, solvent usage, biomass burning, and fuel evaporation. On the other hand, vegetation is the main biogenic source of VOC. In developed areas in China, vehicle exhaust and industrial emissions are the two major VOC sources (He et al., 2019; Hui et al., 2018; Hui et al., 2019; Mo et al., 2017; Song et al., 2018; An et al., 2014; Mozaffar & Zhang, 2020). Vehicle-related sources are more dominant in the North China Plain (NCP), Central China (CC), and Pearl River

Delta (PRD) regions. But industry-related sources are more influential in the Yangtze River Delta (YRD) area (Zhang et al., 2017; Meng et al., 2015; Sun et al., 2019; He et al., 2019; Zhang et al., 2018; An et al., 2017; Mozaffar & Zhang, 2020; Shao et al., 2016). Alkanes, alkenes, aromatics, oxygenated-VOCs (OVOCs), and halocarbons are the most common VOC-groups in the atmosphere (Hui et al., 2019; Hung-Lung et al., 2007; Song et al., 2018; Tiwari et al., 2010; He et al., 2019; Na et al., 2001; Hui et al., 2018). The seasonal change affects VOC concentration and composition. For example, the contribution from biogenic and solvent utilization increases in summer, and the contribution from combustion sources increases in winter (Mo et al., 2017; Song et al., 2018; An et al., 2014). The chemical reactivity of VOCs depends on their chemical composition. For instance, alkenes and aromatics are generally more reactive than alkanes (Carter, 2010). Analysis of OH radical loss rate (L_{OH}) is commonly used to understand the chemical reactivity of VOCs (Hui et al., 2018).

Industries are an important source of VOCs, and different reactive and hazardous VOC emissions from industries have already been reported in different areas of the earth (Zhang et al., 2018; Na et al., 2001; Hung-Lung et al., 2007; Yan et al., 2016; Tiwari et al., 2010; Shi et al., 2015; Zhang et al., 2018b). For instance, Zhang et al. (2018) reported a high concentration of alkanes (21.3±17.8 mg m^{-3} out of the total 23.1±24.5 mg m^{-3})and lifetime cancer risk of different aromatics and halocarbons in a petroleum refinery in Guangzhou, China. A high concentration of OVOCs (829.7±1076.7 ppbC out of a total of 1317.3±1184.5 ppbC) was observed in an industrial area in Ulsan, Korea (Na et al., 2001). Hung-Lung et al. (2007) mentioned a high concentration of aromatics (~90 ppb out of a total of ~160 ppb) in an industrial area in Taiwan. A high concentration of halocarbons (9590.2 mg m^{-3} out of a total of 19652 mg m^{-3}) was observed in an iron smelt plant in Liaoning, China (Shi et al., 2015). Zhang et al. (2018) mentioned a high concentration of alkanes (39.4 ppbv out of a total of 94.15 ppbv) and aromatics (18.9 ppbv out of a total of 94.15 ppbv) in a petrochemical industrial area in Shanghai, China. Therefore, VOC composition varies among the industries/industrial areas in different regions. Mostly, short-term investigations are performed to characterize the VOCs in industry-affected areas. In the current study, we carried out a comprehensive investigation on VOC in an industrial area in Nanjing between July 2018 and May 2020. Several VOC investigations have already been performed in the Nanjing industrial area, but OVOCs and halocarbons were not measured in those studies (An et al., 2017; An et al., 2014).

However, OVOCs and halocarbons are already mentioned as one of the highest concentrated VOC groups in other industrial regions (Na et al., 2001; Shi et al., 2015). In the current study area, a high concentration of alkanes (19.6 ppbv out of the total 43.5 ppbv) and alkenes (11.1 ppbv out of the total 43.5 ppbv) were observed in a previous investigation (An et al., 2014). Besides the incomplete VOC measurements, O_3 formation sensitivity to its precursors was not investigated properly using a photochemical box model in Nanjing. Moreover, source apportionment of VOCs was not conducted for different seasons of a year.

In the current study, we report the variations in concentrations and compositions of VOC during the observation period. We present the possible source areas and potential sources of VOC based on potential source contribution function (PSCF) and positive matrix factorization (PMF) model analysis. We also report the chemical reactivity of the VOC using L_{OH}. We also present the sensitivity analysis of O_3 formation using the empirical kinetic modelling approach (EKMA) and relative incremental reactivity (RIR) analysis. Therefore, this study provides valuable information to the scientific community and policymakers.

2 Material and Methods

2.1 Sampling Site Description, Gases Analysis, and Meteorology Data

Field measurements were carried out at Nanjing University of Information Science and Technology (32.1°N, 118.4°E) for about one month in winter, spring, and summer and three months in autumn between July 2018 and May 2020. The sampling site was on the rooftop of a building (~20 m). The sampling site is surrounded by different chemical and petrochemical industries, steel plants, gas stations, high traffic roads, and residential areas. A detailed description of the sampling site can be found elsewhere (Mozaffar et al., 2020).

We analysed ambient air VOCs using an online GC-FID/MS instrument (AC-GCMS 1000, Guangzhou Hexin Instrument Co., Ltd., China). The FID detector analysed C2-C5 VOCs and the MS analysed C6-C12 VOCs. The instrument analysed one sample every hour. During the investigation period, we

inspected and calibrated the instrument regularly to ensure the accuracy of the data (Mozaffar et al., 2020). We monitored the O_3 concentrations using a 49i O_3 analyser (Thermo Fisher Scientific Inc., USA). NO, NO_2 and NOx concentrations were measured using a 42i NO-NO_2-NOx analyser (Thermo Fisher Scientific Inc., USA). SO_2 concentrations were followed using a 43i SO_2 analyser (Thermo Fisher Scientific Inc., USA) and CO concentrations were measured using a 48i CO analyser (Thermo Fisher Scientific Inc., USA). We also measured temperature and relative humidity, wind speed, wind direction, and solar radiation by HMP155 (Vaisala, Finland), 010C (Met One Instruments, Inc., USA), 020CC (Met One Instruments, Inc., USA), and CNR4 (Kipp & Zonen, The Netherlands) analysers, respectively. A detailed description of the instrumentation, sampling procedure, analysis, quality control, and calibration procedure can be found elsewhere (Mozaffar et al., 2020).

2.2 Positive Matrix Factorization (PMF) model and Potential Source Contribution Function (PSCF)

We used the positive matrix factorization (PMF) model (US Environmental Protection Agency, USEPA, version 5.0) for the source apportionment of VOCs. A detailed description of the model can be found elsewhere (Hui et al., 2019; Song et al., 2018). We used 20 potential VOC tracers (Fig. S1-S4) in the PMF model. The error fraction was set to 20% for the sample data uncertainty estimation. We explored the PMF factor number from 4-8 to determine the optimal number of sources. Finally, we decided to choose a 7 to 8-factor solution for different seasons as Q_{true}/Q_{robust} was ~1.0, $Q_{true}/Q_{expected}$ ranged from 0.99-1.45 (Hui et al., 2019), and strong correlations (0.7-0.8) were observed between the concentrations extracted from the model and the observed concentrations of each compound (He et al., 2019).

We used the potential source contribution function (PSCF) to locate possible source areas of VOCs for different seasons during the investigation period. We used Zefir analysis software to do the PSCF analysis and the Hysplit4 model to cluster the backward trajectories (Petit et al., 2017). Backward trajectories at the sampling site were estimated using the National Centers for Environmental Prediction data (ftp://arlftp.arlhq.noaa.gov/pub/archives/gdas1). We estimated 72 hr backward trajectories 24 times a day arriving at 500 m above the ground surface using the hysplit4 model. For the PSCF analysis, we divided the geographic region covered by the back trajectories into an array of 0. 1° × 0. 1° grid cells

and used the mean TVOCs concentration as the VOC reference value. More details about the PSCF analysis can be found in previous studies (Chen et al., 2018).

2.3 OH radical loss rate (L_{OH})

To evaluate the daytime photochemistry of VOCs, we estimated their OH radical loss rate (L_{OH}). The following equation was used to estimate the L_{OH} (s^{-1}) (Zhang et al., 2020).

$$L_{OH} = [VOC]_i \times k_{OH,i} \quad (1)$$

Where $[VOC]_i$ is the concentration of VOC species i (molecule cm^{-3}), $k_{OH,i}$ (cm^3 $molecule^{-1}$ s^{-1}) is the reaction rate constant of i VOC with the OH radical. The k_{OH} values for the VOCs are collected from Carter (2010) (Table S1).

2.4 Empirical Kinetic Modelling Approach (EKMA) and Relative Incremental Reactivity (RIR)

The empirical kinetic modelling approach (EKMA) is a well-known procedure to develop the O_3 formation reduction strategy by testing the relationship between ambient O_3 and its precursors (He et al., 2019; Hui et al., 2018; Vermeuel et al., 2019; Tan et al., 2018). To obtain data for the EKMA isopleth, we used the Framework for 0-D Atmospheric Model (F0AM v 3.2, Wolfe et al., 2016), a photochemical box model run by Master Chemical Mechanism (MCM) v3.2 chemistry (Jenkin et al., 1997; 2003, 2015; Saunders et al., 2003). The FOAM-MCM box model can simulate 16940 reactions of 5733 chemical species. The box model was run using the VOCs and gas concentrations and the meteorological data as input. 61 VOCs were constrained in the model as the rest of the observed VOC species reactions are not included yet in MCM. These constrained VOCs are listed in Table S1. To generate the O_3 isopleth from the model simulated data, a total of 121 reduction scenarios (11 NOx × 11 VOC concentrations) were simulated and the maximum O_3 produced at each model scenario was saved.

The relative incremental reactivity (RIR, Cardelino & Chameides, 1995) is also used to test the O_3 formation sensitivity of its precursors. We also utilized the FOAM-MCM box model data to estimate the RIR. The RIR is simply defined as the percentage change in O_3 formation per percentage change in

precursor's concentration. In this study, we reduced the precursor concentration by 10% for the RIR estimation. The RIR was estimated using the following equation.

$$RIR\ (X) = \frac{[P_{O_3}(X) - P_{O_3}(X-\Delta X)]/P_{O_3}(X)}{[\Delta X]/[X]} \quad (2)$$

Where [X] is the observed concentration of a precursor X, [ΔX] is the changes in the concentration of X. $P_{O3}(X)$ and $P_{O3}(X- \Delta X)$ are the simulated net O_3 production using the observed and reduced concentration of the precursor X, respectively.

3 Results and discussion

3.1 Overview of the metrological conditions and air pollutants concentrations

The time series of the hourly data is shown in Fig. 1. The discontinuity of the time series data is due to the failure of the instruments and COVID-19 lockdowns. The data measured between July and August 2018 is termed "summertime data". Similarly, data collected between September and November 2018 is "autumntime data", December 2018 and January 2019 is "wintertime data", and April and May 2020 is "springtime data". Overall, the observed temperature and solar radiation gradually decreased from summer to winter and increased back to the summertime level in spring. The temperature ranged between -5.7 and 41.4 °C during the measurement period. The relative humidity values varied from 18 to 100%; high values were generally observed in winter and autumn. During the observation period, wind speeds ranged between 0.1 and 7.5 ms^{-1}. Wind prevailed at the sampling site from many directions during the measurement periods; more details about the wind direction will be discussed in Sect.3.3.2. The O_3 and NOx concentrations varied from 2 to 160 ppbv and 0.4 to 90 ppbv, respectively. Whereas high O_3 concentrations (>80 ppbv) were observed in summer and spring, high NOx concentrations were measured in winter and at the end of autumn. The CO and SO_2 concentrations ranged from 83 to 3398 ppbv and 0.5 to 21 ppbv, respectively. In general, high CO and SO_2 concentrations were observed in the winter and spring. The measured NO and NO_2 concentrations varied from 0.4 to 51 ppbv and 1 to 79 ppbv, respectively. In general, high NO and NO_2 concentrations were observed in autumn and winter. The TVOCs concentrations estimated with all the measured VOCs varied between 9 and 393 ppbv

during the observation period and the high values were measured in autumn and winter. More details about the abovementioned parameters will be discussed in the following section.

3.2 Concentration and composition of VOCs

In total, 100 VOCs were observed in the Nanjing industrial area, including 27 alkanes, 11 alkenes, one alkyne, 17 aromatics, 31 halocarbons, 12 OVOCs, and one other (carbon disulfide) (Table S2). Ethane (5.8±2.5 ppbv), propane (4.2±1.5 ppbv), and ethylene (3±1.6 ppbv) were the most abundant VOCs in the study area during the observation period. However, we observed season-wise variations in the order of abundant VOC species (Table S2). For instance, acetone was the 3rd highest concentrated VOC in spring. The abovementioned 4 VOC species are also frequently mentioned as the most abundant VOCs in different regions in China (Deng et al., 2019; He et al., 2019; J. Li et al., 2018; Ma et al., 2019). We compared the individual VOC concentrations with the available data presented in recent investigations. The individual VOC concentrations in the current observation were similar to those reported in the previous investigation in the same study area (An et al., 2017). However, they were almost twice those found in a nonindustrial suburban area in Nanjing (Wu et al., 2020) (Table S2). Some of the differences may be due to the differences in the observation period. The reported yearly concentrations (Wu et al., 2020) were probably estimated over continuous measurement data for a year. However, in the current observation, the measurements were not continuously performed during all the days of a year. Individual VOC concentrations in the autumn were about 1.4 times lower than those measured in Beijing in October and November (Li et al., 2015). The wintertime individual VOC concentrations were also about 1.4 folds lower than those measured in Shanghai during November-January (Zhang et al., 2018). But, the yearly individual VOC concentrations in the current observation were similar to those measured in Guangzhou from June to May (Zou et al., 2015). During the observation period, the concentrations of different VOC-groups were in the order of alkanes (21±7 ppbv, 35%)> halocarbons (14.3±7.3 ppbv, 24%)> aromatics (9.9±5.8 ppbv, 17%)> OVOCs (7.5±1.9 ppbv, 13%)> alkenes (5±1.9 ppbv, 8%)> alkynes (1.4±0.3 ppbv, 2%)> others (0.5±0.2 ppbv, 1%). Relatively high proportions of halocarbons and aromatics were observed in autumn (25.7 and 19.3%, respectively) and winter (25.8 and 17.6%, respectively) compared to those measured in summer (20.4 and 11.8%, respectively) and

spring (20.3 and 13.6%, respectively) (Fig. 2f). It could be related to the burning of biomass and fossil fuel for additional heating. Similar to the observation in the current study, the alkane family is generally the most abundant VOC group in China (Mozaffar & Zhang, 2020). The relatively high contribution of halocarbons to the TVOCs could be related to the industrial emissions in the study area. However, halocarbons and OVOCs were not measured in previous investigations in the same study area (An et al., 2014; An et al., 2017; Shao et al., 2016) and also in another suburban area in Nanjing (Wu et al., 2020). Either the aromatics or alkenes group was mentioned as the second most abundant VOC group in those studies in Nanjing, which is the 3rd and 5th most abundant VOC group in the current investigation. The TVOCs concentration estimated with all the measured VOCs was 59.8±28.6 ppbv over the whole observation period, and relatively higher TVOCs concentrations were measured in autumn (83±20 ppbv) and winter (77.5±16.8 ppbv) compared to those observed in spring (39.6±13.1 ppbv) and summer (38.8±10.2 ppbv). The TVOCs concentrations without halocarbons were 45.4±20.4, 61.7±14.6, 57.4±11.8, 31.6±10.9, and 30.9±8.2 ppbv during the whole observation period, autumn, winter, spring, and summer, respectively. As mentioned before, halocarbons and OVOCs were not reported in the previous investigations in Nanjing (An et al., 2017; Wu et al., 2020). The current TVOCs concentration without halocarbons and OVOCs was similar to the previous investigation in the same study area, however, 2-folds higher than the one reported in the nonindustrial suburban area in Nanjing. The diurnal variation of the TVOCs, alkenes, aromatics, halocarbons, OVOCs, and alkanes concentrations showed a double-hump structure (Fig. 2a, b, d, & e). This double-hump pattern indicates the contribution of traffic emissions during the rush hours in the morning and evening. The lowest concentration of the TVOCs and different VOC groups reached 12:00-16:00. Oppositely, the highest concentration of O_3 was reached in that period (Fig. 3). The lowest O_3 concentrations were observed in winter, which was consistent with the solar radiation.

3.3 Sources of VOCs

3.3.1 Potential Source Contribution Function (PSCF)

Besides the local sources, both the long-distance and short-distance transport of air mass could bring VOCs to the study area. Figure 4 shows the wind cluster and PSCF analysis results for different

seasons. During summer, the major air masses were short-distance transport from the south (44%) direction and two long-distance types of transport from the southeast (31 and 25%) direction. High PSCF values were in the nearby south and southeast directions; therefore, VOC pollution in the study area was mainly affected by short-distance transport from the south and east directions. During autumn, the dominant air masses were short-distance transport from the northwest (35%) and long-distance transport from the north (34%) directions. However, according to the PSCF analysis, VOC pollution was mainly influenced by the short distance transport from the south direction. During winter, short-distance transport from the northwest (52%) direction was the major incoming air masses to the study area. According to the PSCF values, the short-distance air masses from the south and north mainly transported VOC to the receptor site. During the spring, air masses were primarily transported from the north (50%) and the southwest (32%). A minor long-distance air mass was transported from the northwest (18%) direction. Atmospheric VOCs were mainly transported by these air masses to the study site, mostly from the nearby areas. Overall, the high PSCF values were concentrated around the measurement site. Therefore, short-distance transport from the surrounding areas and cities was the main reason for the high VOC concentration. The above conclusion perfectly makes sense as the sampling site is surrounded by different chemical and petrochemical industries, steel plants, gas stations, high traffic roads, and residential areas.

3.3.2 PMF Model Analysis

According to the PMF model analysis, five VOC sources were common during all the measurement seasons. They were biomass/biofuel burning, LPG/NG usage, gasoline evaporation, gasoline vehicle exhaust, and paint solvent usage (Sect. S1). The biogenic source was distinguished only in the summer. Figure 5 shows the relative contributions of different sources to ambient VOCs during different seasons. Overall, vehicle-related sources contributed the most to the ambient VOC concentrations. The total contributions of vehicle-related emissions were about 39%, 33%, 48%, and 42% in summer, autumn, winter, and spring, respectively. The contributions of biomass/biofuel burning sources were about 19%, 21%, 17%, and 16.4% in summer, autumn, winter, and spring, respectively. Besides these two sources,

LPG/NG usage (18%, 21%, 16%, and 18%, respectively) and paint solvent usage (8%, 12%, 11%, 5%, respectively) were two other important VOC sources during those four seasons.

3.4 Chemical reactivity (L_{OH})

The estimated loss rates of OH radical (L_{OH}) with VOCs were about 2-fold high in autumn (13.7 s^{-1}) and winter (13.5 s^{-1}) compared to those in summer (7 s^{-1}) and spring (7.5 s^{-1}) (Fig. 6 a). The relatively high L_{OH} values in autumn and winter were due to the relatively high VOC concentrations in these seasons (Fig.2). The average L_{OH} value was 10.4±3.6 s^{-1} over the four seasons. It was in a similar range to the values determined in Guangzhou (10.9 s^{-1}), Chongqing (10 s^{-1}), Xian (1.6-16.2 s^{-1}), and Tokyo (7.7-13.4 s^{-1}), but higher than the values estimated in Shanghai (2.9-5 s^{-1}, 6.2 s^{-1}) and Beijing (7 s^{-1}) (Tan et al., 2019; Zhu et al., 2019; Yoshino et al., 2012; Song et al., 2020). While alkene was the highest contributor to the L_{OH} in summer (3 s^{-1}, 43%) and spring (2.6 s^{-1}, 35%), aromatic was the maximum contributor in autumn (6.9 s^{-1}, 50%) and winter (5.9 s^{-1}, 44%) (Fig. 6 a & d). An increase in the OH loss rate by OVOCs was observed in spring (17%) compared to the other seasons (10, 8, and 9% in summer, autumn, and winter, respectively). Over the four seasons, the contribution of VOC groups to L_{OH} exhibited the following trend: aromatics > alkenes > alkanes > OVOCs > halocarbons. Similar to the current study, the aromatic group is also mentioned as the maximum contributor to L_{OH} in different regions in China. However, the alkene group is generally reported as the top contributor to L_{OH} (Zhang et al., 2020; Zhao et al., 2020; Hui et al., 2018; Song et al., 2020). Figure 6 also shows the top 10 VOCs contributing to L_{OH} for different seasons. Whereas isoprene was the highest contributor to L_{OH} in summer, it was styrene in autumn and winter. On the other hand, naphthalene was the main contributor to L_{OH} in the spring. Overall, styrene, naphthalene, ethylene, and isoprene were the main contributors to L_{OH}. In previous studies in China, these compounds are also mentioned as one of the highest contributors to L_{OH} (Zhao et al., 2020; Hui et al., 2018; Song et al., 2020).

3.5 Sensitivity analysis of O_3 formation

Figure 7 shows the EKMA isopleth diagrams of O_3 for different seasons. In all the diagrams, VOC and NOx = 100 % is the base case. The ridgeline divided the diagrams into two regimes, VOC-sensitive

above the line and NOx-sensitive below the line. For all the seasons, the study area fell above the ridgeline. Moreover, O_3 production decreased with the decrease in VOC concentration. Therefore, the study area was in the VOC-sensitive regime for O_3 formation during all the seasons. As a case study, O_3 formation sensitivity to its precursors was tested on a high O_3 concentration day (July 29 2018, maximum 126 ppbv). During the high O_3 episode, the study area was also in the VOC-sensitive regime for O_3 formation (Fig. S5). We also employed the RIR analysis to evaluate the O_3 production sensitivity to VOC, NOx, and CO concentrations (Fig. 8). The RIR value of VOC was the highest during all the seasons. It indicates that O_3 production was more sensitive to the reduction of VOC concentration. This finding is consistent with the EKMA isopleth diagrams (Fig. 7). Except for the spring, the RIR values of CO were very small relative to those for the VOC. It indicates that the CO concentrations were relatively less important for the O_3 formation during those seasons. The RIR values for NOx were negative during all the seasons, implying that the O_3 formation was in the NOx-titration regime in the study area. From the above analysis, it is evident that a reduction of VOC concentration in the study area will be the most efficient way to reduce the O_3 formation. The previous two studies performed in Nanjing also concluded with the same finding based on VOC/NOx ratios and RIR analysis (An et al., 2015; Xu et al., 2017). Our findings are also consistent with the previous studies performed in other regions of China (Tan et al., 2018a; He et al., 2019; Feng et al., 2019; Ma et al., 2019). However, NOx-sensitive regions for O_3 formation are also found in China (Tan et al., 2018; Jia et al., 2016).

4 Conclusions

Nanjing is one of the biggest industrial cities in China. We performed a long-term investigation of ambient VOCs in Nanjing. Compared to the previous investigation in the current study area, similar TVOCs concentrations were observed. However, about 2-folds higher TVOCs concentrations were observed compared to the one previously reported in a nonindustrial suburban area in Nanjing. TVOCs concentrations were about twice as high in autumn and winter compared to those observed in summer and spring. Generally, haze pollution occurs most frequently in autumn and winter. Therefore, VOC concentration reduction in these seasons is an important step to reduce haze pollution in the study area. The halocarbon group was the 2nd largest contributor to the TVOCs following alkanes, indicating the

impact of industrial emissions on the local air. As halocarbons are carcinogenic, their emissions need to be reduced. The short-distance air mass from the surrounding areas and cities was the main reason for the high VOC concentration. Hence, local emissions need to be reduced. Vehicle-related emissions were the major VOC source in the study area, thus, emission reduction from this source should get more priority. Aromatics and alkenes were the major contributors to the L_{OH}. Therefore, these 2 VOC groups should get more priority in emission reduction policies and strategies. During all the seasons, the study area was in the VOC-sensitive regime for O_3 formation. Therefore, VOC emission reduction is the most effective way to decrease the local O_3 formation.

Data availability

All the data presented in this article can be accessed through https://osf.io/bm6cs/.

Author contribution

YLZ designed and supervised the project; MYF, FX, YCL, FC, and AM conducted the measurements; AM analysed the data and prepared the manuscript. All authors contributed in discussion to improve the article.

Competing interests

The authors declare that they have no conflict of interest.

Acknowledgements

The authors thank funding support from the National Nature Science Foundation of China (No. 41977305), the Provincial Natural Science Foundation of Jiangsu (No. BK20180040), and the Jiangsu Innovation & Entrepreneurship Team. We are also grateful to Zijin Zhang and Meng-Yao Cao for their help on sampling.

References

An, J., Wang, J., Zhang, Y., & Zhu, B.: Source Apportionment of Volatile Organic Compounds in an Urban Environment at the Yangtze River Delta, China, Archives of Environmental Contamination and Toxicology, 72(3), 335–348, https://doi.org/10.1007/s00244-017-0371-3, 2017.

An, J., Zhu, B., Wang, H., Li, Y., Lin, X., & Yang, H.: Characteristics and source apportionment of VOCs measured in an industrial area of Nanjing, Yangtze River Delta, China, Atmospheric Environment, 97, 206–214, https://doi.org/10.1016/j.atmosenv.2014.08.021, 2014.

An, J., Zou, J., Wang, J., Lin, X., & Zhu, B.: Differences in ozone photochemical characteristics between the megacity Nanjing and its suburban surroundings, Yangtze River Delta, China, Environmental Science and Pollution Research, 22(24), 19607–19617, https://doi.org/10.1007/s11356-015-5177-0, 2015.

Cardelino, C. A., & Chameides, W. L.: An observation-based model for analyzing ozone precursor relationships in the urban atmosphere, Journal of the Air and Waste Management Association, 45(3), 161–180, https://doi.org/10.1080/10473289.1995.10467356, 1995.

Carter, W. P. L.: Development of the SAPRC-07 chemical mechanism, Atmospheric Environment, 44(40), 5324–5335, https://doi.org/10.1016/j.atmosenv.2010.01.026, 2010.

Chen, Y., Ge, X., Chen, H., Xie, X., Chen, Y., Wang, J., … Chen, M. : Seasonal light absorption properties of water-soluble brown carbon in atmospheric fine particles in Nanjing, China, Atmospheric Environment, 187(June), 230–240, https://doi.org/10.1016/j.atmosenv.2018.06.002, 2018.

Deng, Y., Li, J., Li, Y., Wu, R., & Xie, S. : Characteristics of volatile organic compounds, NO2, and effects on ozone formation at a site with high ozone level in Chengdu, Journal of Environmental Sciences (China), 75(2), 334–345, https://doi.org/10.1016/j.jes.2018.05.004, 2019.

Feng, R., Wang, Q., Huang, C. chen, Liang, J., Luo, K., Fan, J. ren, & Zheng, H. J. : Ethylene, xylene, toluene and hexane are major contributors of atmospheric ozone in Hangzhou, China, prior to the 2022

Asian Games, Environmental Chemistry Letters, 17(2), 1151–1160, https://doi.org/10.1007/s10311-018-00846-w, 2019.

Feng, T., Bei, N., Huang, R. J., Cao, J., Zhang, Q., Zhou, W., … Li, G. : Summertime ozone formation in Xi'an and surrounding areas, China, Atmospheric Chemistry and Physics, 16(7), 4323–4342, https://doi.org/10.5194/acp-16-4323-2016, 2016.

He, Z., Wang, X., Ling, Z., Zhao, J., Guo, H., Shao, M., & Wang, Z. : Contributions of different anthropogenic volatile organic compound sources to ozone formation at a receptor site in the Pearl River Delta region and its policy implications, Atmospheric Chemistry and Physics, 19(13), 8801–8816, https://doi.org/10.5194/acp-19-8801-2019, 2019.

Hui, L., Liu, X., Tan, Q., Feng, M., An, J., Qu, Y., … Cheng, N.: VOC characteristics, sources and contributions to SOA formation during haze events in Wuhan, Central China, Science of the Total Environment, 650, 2624–2639, https://doi.org/10.1016/j.scitotenv.2018.10.029, 2019.

Hui, L., Liu, X., Tan, Q., Feng, M., An, J., Qu, Y., … Jiang, M. : Characteristics, source apportionment and contribution of VOCs to ozone formation in Wuhan, Central China, Atmospheric Environment, 192(August), 55–71, https://doi.org/10.1016/j.atmosenv.2018.08.042, 2018.

Hung-Lung, C., Jiun-Horng, T., Shih-Yu, C., Kuo-Hsiung, L., & Sen-Yi, M. : VOC concentration profiles in an ozone non-attainment area: A case study in an urban and industrial complex metroplex in southern Taiwan, Atmospheric Environment, 41(9), 1848–1860, https://doi.org/https://doi.org/10.1016/j.atmosenv.2006.10.055, 2007.

Jenkin, M. E., Young, J. C., & Rickard, A. R. : The MCM v3.3.1 degradation scheme for isoprene, Atmospheric Chemistry and Physics, 15(20), 11433–11459, https://doi.org/10.5194/acp-15-11433-2015, 2015.

Jenkin, Michael E., Saunders, S. M., & Pilling, M. J. : The tropospheric degradation of volatile organic compounds: A protocol for mechanism development, Atmospheric Environment, 31(1), 81–104, https://doi.org/10.1016/S1352-2310(96)00105-7, 1997.

Jia, C., Mao, X., Huang, T., Liang, X., Wang, Y., Shen, Y., … Gao, H.: Non-methane hydrocarbons (NMHCs) and their contribution to ozone formation potential in a petrochemical industrialized city, Northwest China, Atmospheric Research, 169, 225–236. https://doi.org/10.1016/j.atmosres.2015.10.006, 2016.

Li, J., Xie, S. D., Zeng, L. M., Li, L. Y., Li, Y. Q., & Wu, R. R. : Characterization of ambient volatile organic compounds and their sources in Beijing, before, during, and after Asia-Pacific Economic Cooperation China 2014, Atmospheric Chemistry and Physics, 15(14), 7945–7959, https://doi.org/10.5194/acp-15-7945-2015, 2015.

Li, Jing, Zhai, C., Yu, J., Liu, R., Li, Y., Zeng, L., & Xie, S. : Spatiotemporal variations of ambient volatile organic compounds and their sources in Chongqing, a mountainous megacity in China, Science of the Total Environment, 627, 1442–145, https://doi.org/10.1016/j.scitotenv.2018.02.010, 2018.

Ma, Z., Liu, C., Zhang, C., Liu, P., Ye, C., Xue, C., … Mu, Y. : The levels , sources and reactivity of volatile organic compounds in a typical urban area of Northeast China, Journal of Environmental Sciences, 79, 121–134, https://doi.org/10.1016/j.jes.2018.11.015, 2019.

Meng, H. A. N., Xueqiang, L. U., Chunsheng, Z., Liang, R. A. N., & Suqin, H. A. N.: Characterization and Source Apportionment of Volatile Organic Compounds in Urban and Suburban Tianjin , China, Advances in Atmospheric Sciences, 32(3), 439–444, https://doi.org/10.1007/s00376-014-4077-4.1, 2015.

Mo, Z., Shao, M., Lu, S., Niu, H., Zhou, M., & Sun, J.: Characterization of non-methane hydrocarbons and their sources in an industrialized coastal city , Yangtze River Delta , China, Science of the Total Environment, 593–594, 641–653, https://doi.org/10.1016/j.scitotenv.2017.03.123, 2017.

Mozaffar, A., & Zhang, Y. L.: Atmospheric Volatile Organic Compounds (VOCs) in China: a Review, Current Pollution Reports, 6(3), 250–263, https://doi.org/10.1007/s40726-020-00149-1, 2020.

Mozaffar, A., Zhang, Y. L., Fan, M., Cao, F., & Lin, Y. C.: Characteristics of summertime ambient VOCs and their contributions to O3 and SOA formation in a suburban area of Nanjing, China, Atmospheric Research, 240(February), https://doi.org/10.1016/j.atmosres.2020.104923, 2020.

Na, K., Kim, Y. P., Moon, K.-C., Moon, I., & Fung, K.: Concentrations of volatile organic compounds in an industrial area of Korea, Atmospheric Environment, 35(15), 2747–2756, https://doi.org/https://doi.org/10.1016/S1352-2310(00)00313-7, 2001.

Petit, J. E., Favez, O., Albinet, A., & Canonaco, F.: A user-friendly tool for comprehensive evaluation of the geographical origins of atmospheric pollution: Wind and trajectory analyses, Environmental Modelling and Software, 88, 183–187, https://doi.org/10.1016/j.envsoft.2016.11.022, 2017.

Saunders, S. M., Jenkin, M. E., Derwent, R. G., & Pilling, M. J. : Protocol for the development of the Master Chemical Mechanism, MCM v3 (Part A): Tropospheric degradation of non-aromatic volatile organic compounds, Atmospheric Chemistry and Physics, 3(1), 161–180, https://doi.org/10.5194/acp-3-161-2003, 2003.

Shao, P., An, J., Xin, J., Wu, F., Wang, J., Ji, D., & Wang, Y.: Source apportionment of VOCs and the contribution to photochemical ozone formation during summer in the typical industrial area in the Yangtze River Delta, China, Atmospheric Research, 176–177, 64–74, https://doi.org/10.1016/j.atmosres.2016.02.015, 2016.

Shi, J., Deng, H., Bai, Z., Kong, S., Wang, X., Hao, J., … Ning, P.: Emission and profile characteristic of volatile organic compounds emitted from coke production, iron smelt, heating station and power plant in Liaoning Province, China, Science of the Total Environment, 515–516(x), 101–108, https://doi.org/10.1016/j.scitotenv.2015.02.034, 2015.

Song, M., Li, X., Yang, S., Yu, X., Zhou, S., Yang, Y., … Zhang, Y. : Spatiotemporal Variation, Sources, and Secondary Transformation Potential of VOCs in Xi'an, China, 30(August), Atmospheric Chemistry and Physics, 21, 4939–4958, https://doi.org/10.5194/acp-21-4939-2021, 2021.

Song, M., Tan, Q., Feng, M., Qu, Y., & Liu, X.: Source Apportionment and Secondary Transformation of Atmospheric Nonmethane Hydrocarbons in Chengdu , Southwest China, Journal of Geophysical Research Atmospheres, 123(2), 9741–9763, https://doi.org/10.1029/2018JD028479, 2018.

Sun, J., Shen, Z., Zhang, Y., Zhang, Z., Zhang, Q., Zhang, T., … Li, X.: Urban VOC profiles, possible sources, and its role in ozone formation for a summer campaign over Xi'an, China, Environmental Science and Pollution Research, 26(27), 27769–27782, https://doi.org/10.1007/s11356-019-05950-0, 2019.

Tan, Z., Lu, K., Dong, H., Hu, M., Li, X., Liu, Y., … Zhang, Y. : Explicit diagnosis of the local ozone production rate and the ozone-NOx-VOC sensitivities, Science Bulletin, 63(16), 1067–1076, https://doi.org/10.1016/j.scib.2018.07.001, 2018.

Tan, Z., Lu, K., Jiang, M., Su, R., Dong, H., Zeng, L., … Zhang, Y. : Exploring ozone pollution in Chengdu, southwestern China: A case study from radical chemistry to O3-VOC-NOx sensitivity, Science of The Total Environment, 636, 775–786, https://doi.org/10.1016/J.SCITOTENV.2018.04.286, 2018.

Tan, Z., Lu, K., Jiang, M., Su, R., Wang, H., Lou, S., … Zhang, Y.: Daytime atmospheric oxidation capacity in four Chinese megacities during the photochemically polluted season: A case study based on box model simulation, Atmospheric Chemistry and Physics, 19(6), 3493–3513, https://doi.org/10.5194/acp-19-3493-2019, 2019.

Tiwari, V., Hanai, Y., & Masunaga, S.: Ambient levels of volatile organic compounds in the vicinity of petrochemical industrial area of Yokohama, Japan, Air Quality, Atmosphere and Health, 3(2), 65–75, https://doi.org/10.1007/s11869-009-0052-0, 2010.

Vermeuel, M. P., Novak, G. A., Alwe, H. D., Hughes, D. D., Kaleel, R., Dickens, A. F., … Bertram, T. H.: Sensitivity of Ozone Production to NOx and VOC Along the Lake Michigan Coastline, Journal of Geophysical Research: Atmospheres, 124(20), 10989–11006, https://doi.org/10.1029/2019JD030842, 2019.

Wolfe, G. M., Marvin, M. R., Roberts, S. J., Travis, K. R., & Liao, J.: The framework for 0-D atmospheric modeling (F0AM) v3.1, Geoscientific Model Development, 9(9), 3309–3319, https://doi.org/10.5194/gmd-9-3309-2016, 2016.

Wu, R., Zhao, Y., Zhang, J., & Zhang, L.: Variability and sources of ambient volatile organic compounds based on online measurements in a suburban region of nanjing, eastern China, Aerosol and Air Quality Research, 20(3), 606–619, https://doi.org/10.4209/aaqr.2019.10.0517, 2020.

Xu, Z., Huang, X., Nie, W., Chi, X., & Xu, Z.: Influence of synoptic condition and holiday effects on VOCs and ozone production in the Yangtze River Delta region , China, Atmospheric Environment, 168, 112–124, https://doi.org/10.1016/j.atmosenv.2017.08.035, 2017.

Yan, Y., Yang, C., Peng, L., Li, R., & Bai, H.: Emission characteristics of volatile organic compounds from coal-, coal gangue-, and biomass-fired power plants in China, Atmospheric Environment, 143, 261–269, https://doi.org/10.1016/j.atmosenv.2016.08.052, 2016.

Yoshino, A., Nakashima, Y., Miyazaki, K., Kato, S., Suthawaree, J., Shimo, N., … Kajii, Y.: Air quality diagnosis from comprehensive observations of total OH reactivity and reactive trace species in urban central Tokyo, Atmospheric Environment, 49, 51–59, https://doi.org/10.1016/j.atmosenv.2011.12.029, 2012.

Zhang, F., Shang, X., Chen, H., Xie, G., Fu, Y., Wu, D., … Chen, J.: Significant impact of coal combustion on VOCs emissions in winter in a North China rural site, Science of the Total Environment, 720, 137617, https://doi.org/10.1016/j.scitotenv.2020.137617, 2020.

Zhang, H., Li, H., Zhang, Q., Zhang, Y., Zhang, W., Wang, X., … Xia, F. : Atmospheric volatile organic compounds in a typical urban area of beijing: Pollution characterization, health risk assessment and source apportionment, Atmosphere, 8(3), 61, https://doi.org/10.3390/atmos8030061, 2017.

Zhang, Y., Li, R., Fu, H., Zhou, D., & Chen, J.: Observation and analysis of atmospheric volatile organic compounds in a typical petrochemical area in Yangtze River, Journal of Environmental Sciences, 71, 233–248, https://doi.org/10.1016/j.jes.2018.05.027, 2018.

Zhang, Z., Yan, X., Gao, F., Thai, P., Wang, H., Chen, D., … Wang, B. : Emission and health risk assessment of volatile organic compounds in various processes of a petroleum refinery in the Pearl River Delta, Environmental Pollution, 238, 452–461, https://doi.org/10.1016/j.envpol.2018.03.054, 2018.

Zhao, R., Dou, X., Zhang, N., Zhao, X., Yang, W., Han, B., … Bai, Z.: The characteristics of inorganic gases and volatile organic compounds at a remote site in the Tibetan Plateau, Atmospheric Research, 234(October 2019), 104740, https://doi.org/10.1016/j.atmosres.2019.104740, 2020.

Zhu, J., Wang, S., Wang, H., Jing, S., Lou, S., Saiz-Lopez, A., & Zhou, B.: Observationally constrained modelling of atmospheric oxidation capacity and photochemical reactivity in Shanghai, China, Atmospheric Chemistry and Physics, 20, 1217–1232, https://doi.org/10.5194/acp-2019-711, 2020.

Zou, Y., Deng, X. J., Zhu, D., Gong, D. C., Wang, H., Li, F., … Wang, B. G. : Characteristics of 1 year of observational data of VOCs, NOx and O3 at a suburban site in Guangzhou, China, Atmospheric Chemistry and Physics, 15(12), 6625–6636, https://doi.org/10.5194/acp-15-6625-2015, 2015.

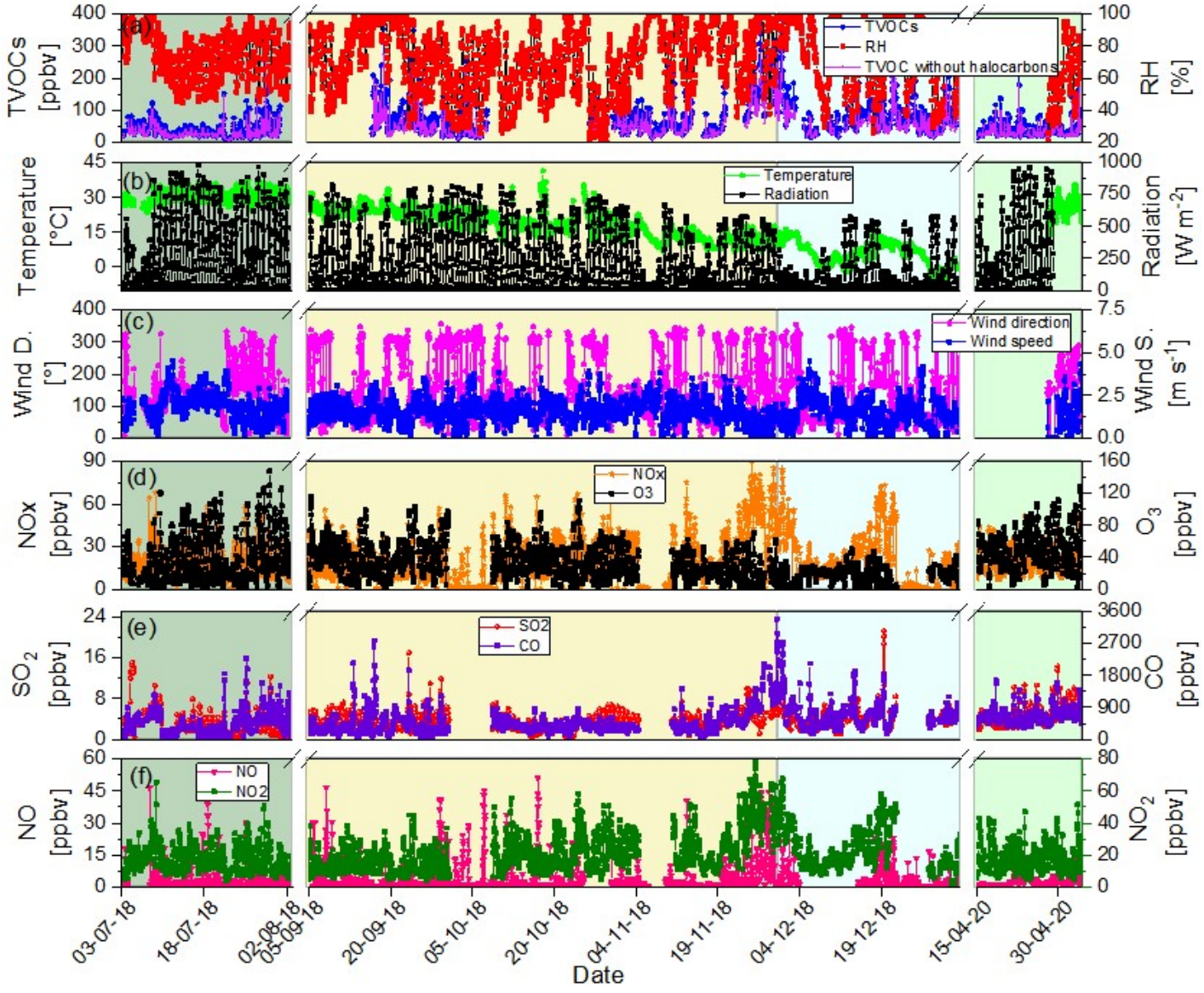

Figure 1: Time series of hourly meteorological parameters, inorganic air pollutants, TVOCs, and TVOCs without halocarbons concentrations during the observation period at Nanjing. The green, yellow, cyan, and light-green shaded areas indicate summer, autumn, winter, and spring seasons, respectively. The discontinuity of the measured data is due to the instruments failure.

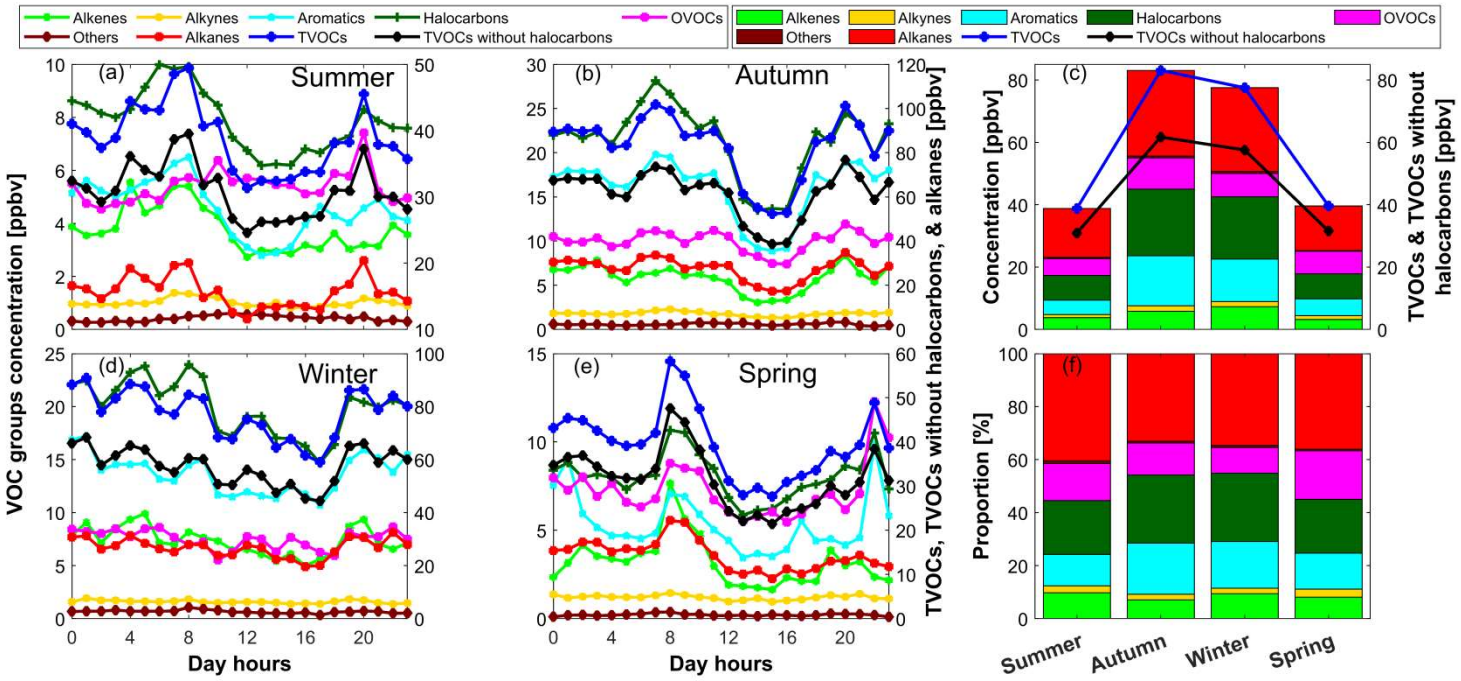

Figure 2: Diurnal variations in different VOC-groups, TVOCs, TVOCs without halocarbons concentrations in different seasons (a, b, d, & e) and seasonal variations in average concentrations and proportion of different VOC-groups, TVOCs, TVOCs without halocarbons (c & f).

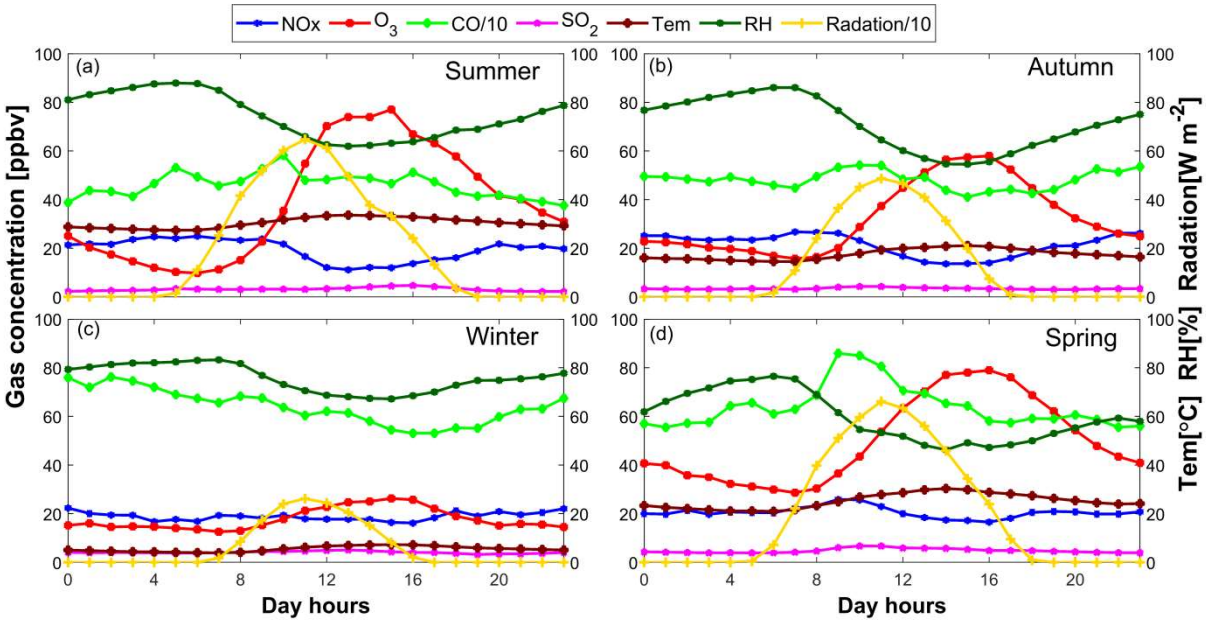

Figure 3: Diurnal variations in weather conditions and NOx, O3, CO, and SO2 concentrations in different seasons. Note that the plotted CO concentrations and solar radiation values are reduced by 10-folds for a better visualization.

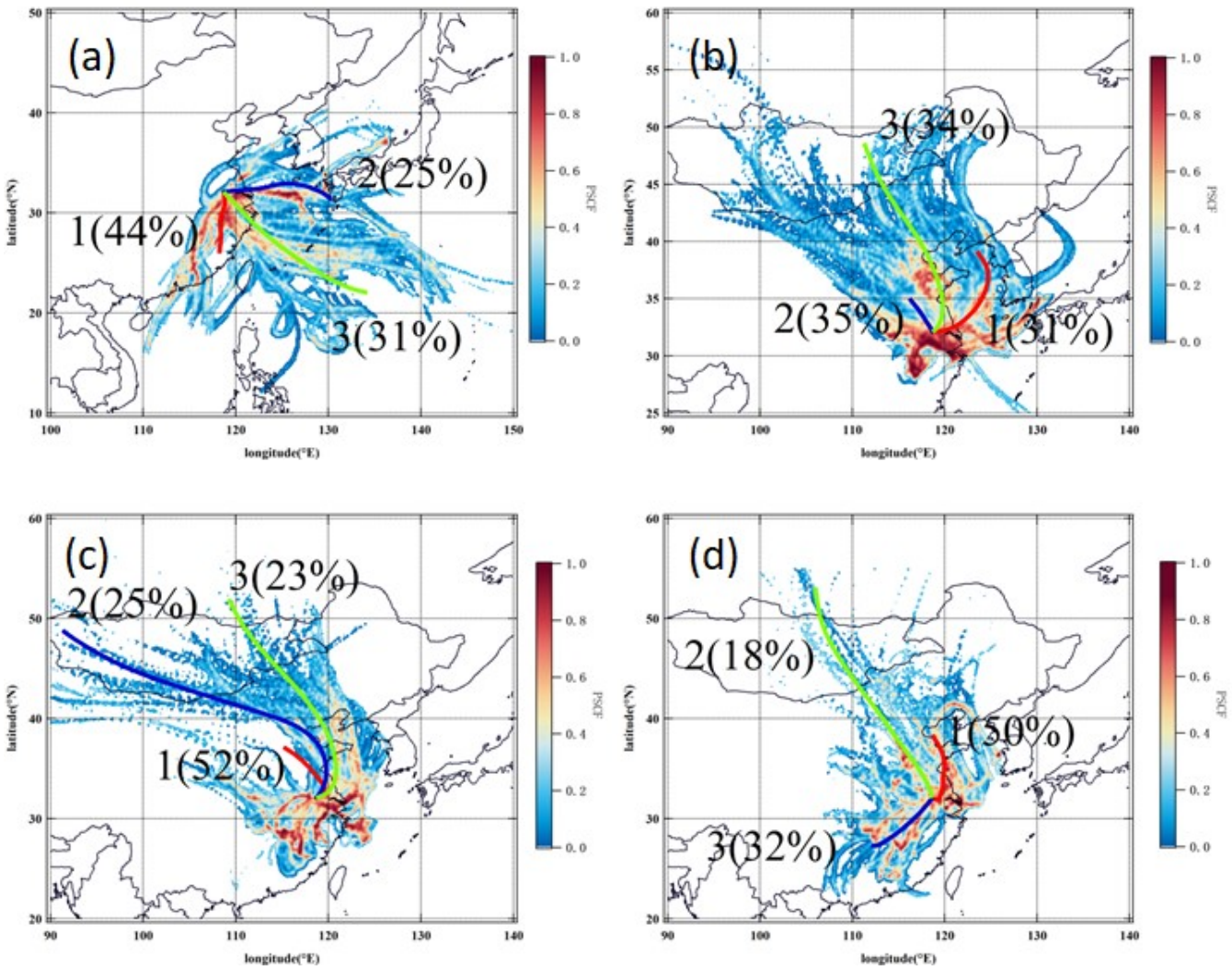

530 **Figure 4: Wind cluster and PSCF analysis during (a) summer (b) autumn, (c) winter, and (d) spring based on the 72 hours backward air mass trajectories from the study area.**

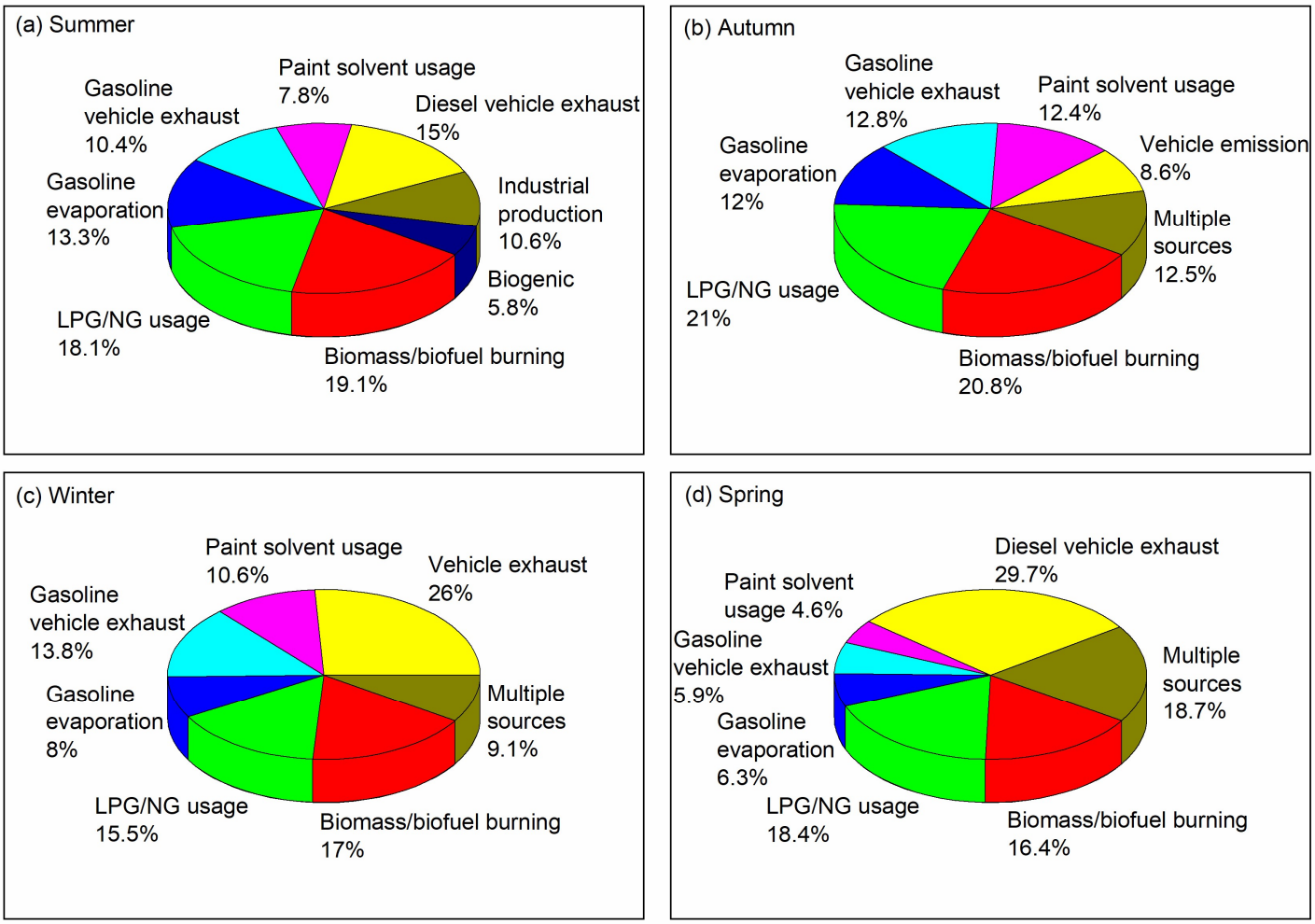

Figure 5: relative contributions of different sources to ambient VOCs in Nanjing industrial area during different seasons

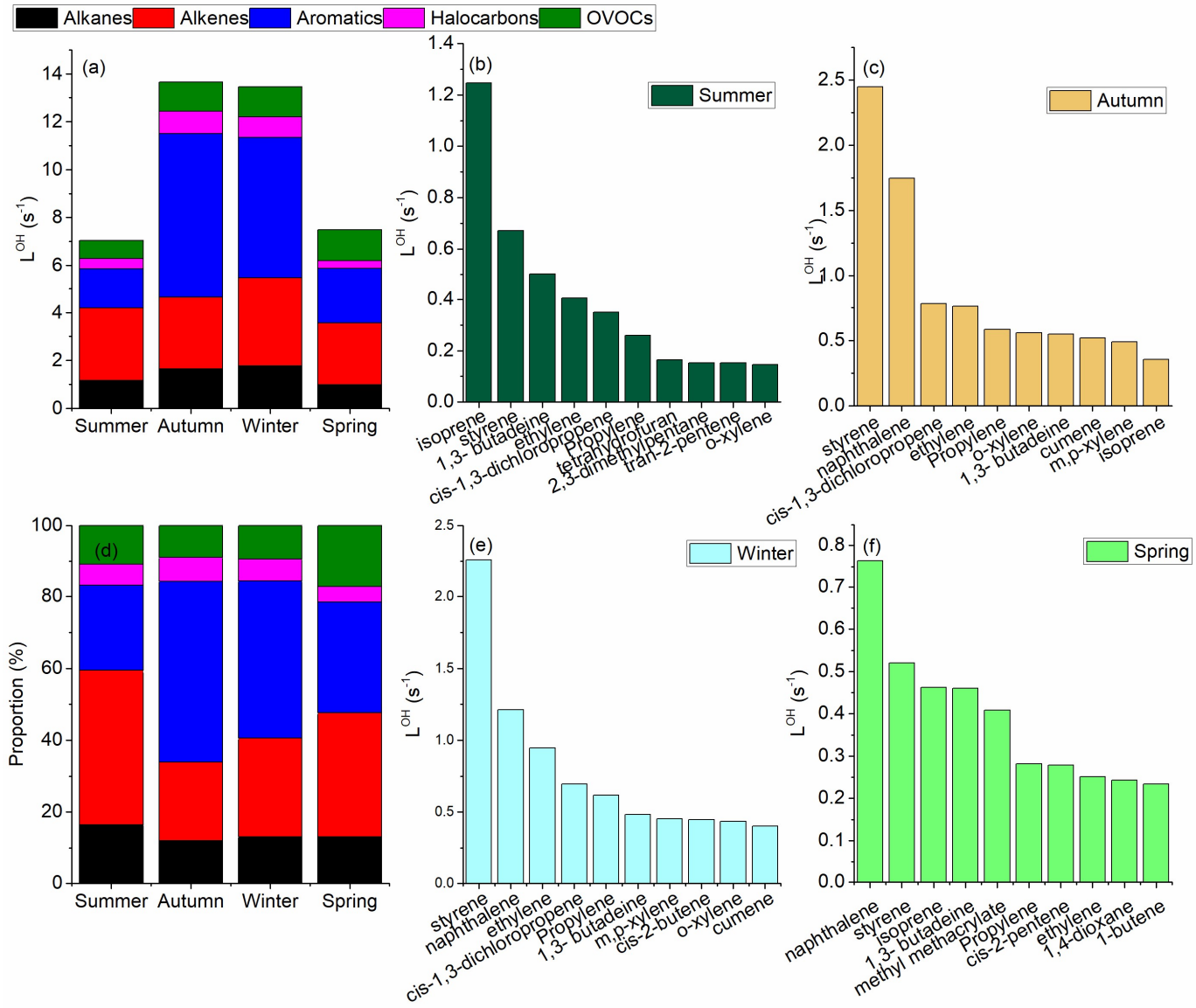

Figure 6: Contribution to OH loss rates of different VOC-groups and the top 10 VOC species in different seasons

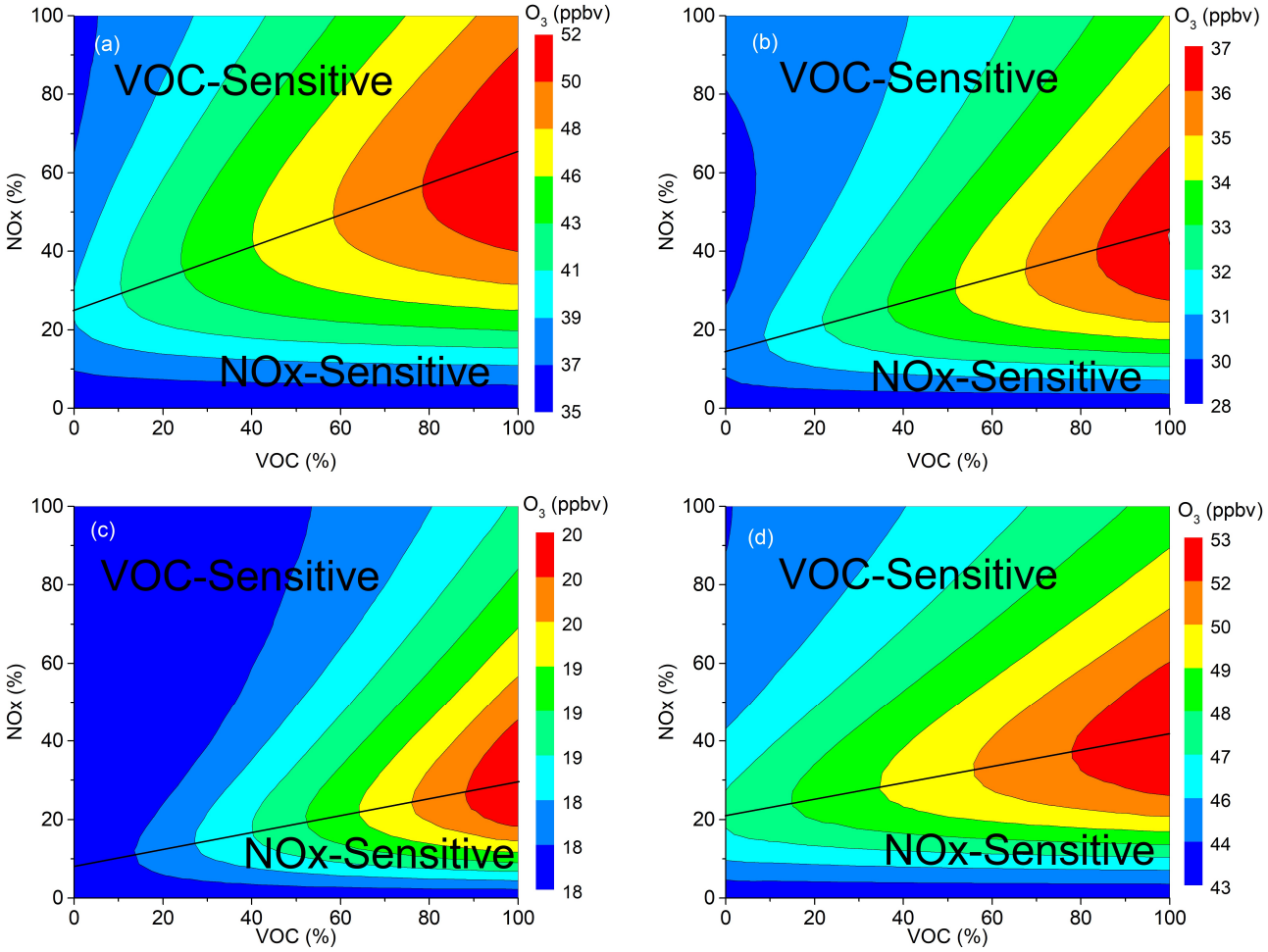

545 **Figure 7: O_3 isopleth diagram for (a) summer (b) autumn, (c) winter, and (d) spring based on percentage changes in VOCs and NOx concentrations in Nanjing and corresponding modelled O_3 production.**

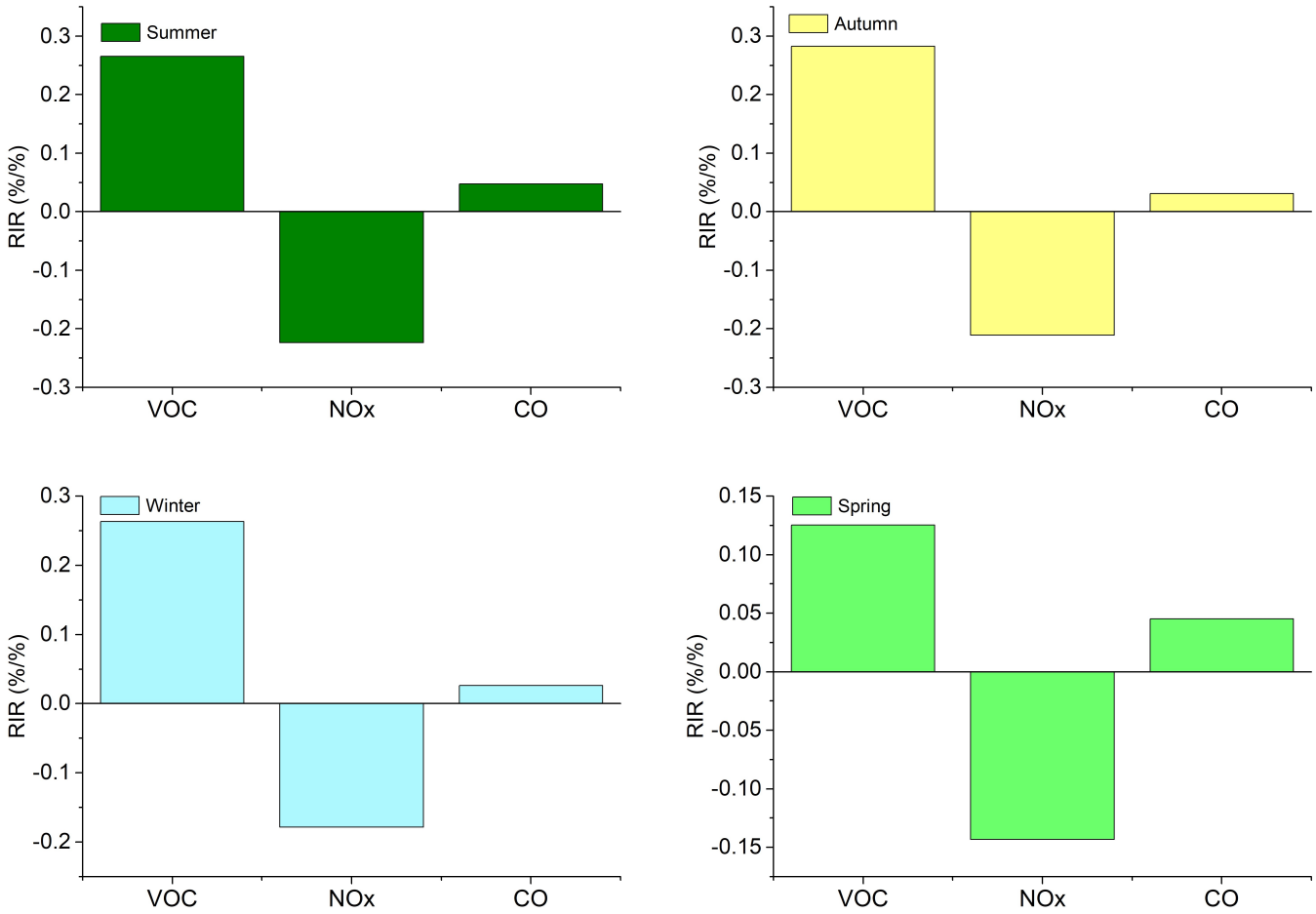

Figure 8: The RIR values of the VOC, NOx, and CO for the different seasons in Nanjing